Materials Science-Poland, 41(2), 2023, pp. 311-324
http://www.materialsscience.pwr.wroc.pl/
DOI: 10.2478/msp-2023-0021

Simulation of the influence of cutting speed and feed rate on tool life in hard turning of AISI 4140 steel

Phacharadit Paengchit[1], Charnnarong Saikaew[2,*]

[1]Department of Industrial Technology, Faculty of Industrial Education, Rajamangala University of Technology Krungthep, Bangkok 10120 Thailand

[2]Department of Industrial Engineering, Faculty of Engineering, Khon Kaen University, Khon Kaen 40002 Thailand

Tool life performances of Al_2O_3+TiC and TiN+AlCrN tool inserts were investigated experimentally under different cutting conditions in turning AISI 4140 steel. The tool life model is defined in accordance with a maximum surface roughness of 0.8 μm for the tool life criterion. The relationships between machining factors (i.e., cutting speed and feed rate) and tool life were obtained by Taylor's formular. The sensitivity of cutting speed and feed rate to tool life was evaluated by Monte Carlo simulation. The results showed that turning with high cutting speeds and feed rates decreased the tool life of both inserts. At different cutting speeds and feed rates, Al_2O_3+TiC exhibited better tool life performance than TiN+AlCrN. In addition, the simulation results indicated the average tool life of Al_2O_3+TiC was approximately 40% greater than that of TiN+AlCrN by varying cutting speeds below and above the cutting speed of 220 m/min while keeping the feed rate constant at 0.06 mm/rev. Similarly, when keeping the cutting speed constant at 220 m/min, the average tool life of Al_2O_3+TiC was approximately 45% greater than that of TiN+AlCrN by varying feed rates below and above the feed rate of 0.06 mm/rev. Variations of tool life values by varying cutting speeds were more sensitive than those by varying feed rates for both tool inserts.

Keywords: *Monte Carlo simulation, surface roughness, cutting speed, feed rate, tool life*

1. Introduction

Tool life is the time during which a tool has cut satisfactorily. Tool life is highly important in cutting processes, which include sawing, turning, milling, drilling, grinding, and broaching, because considerable time and cost have been lost from replacing and resetting cutting tools. Generally, the tool life model is developed by applying Taylor's tool life equation on the basis of the tool wear criterion because it is straightforward to measure quantitively. Taylor's tool life is commonly employed to predict the tool life of drilling tools. For example, John et al. [1] proposed a modified Taylor's tool life equation for high-speed steel tools when drilling polypropylene-based, natural fiber-reinforced composites. Moreover, Farid et al. [2] reported Taylor's tool life equation on the basis of the criterion of 100-μm flank wear at an outer corner while high-speed drilling of A383 Al-Si alloy using uncoated, TiAlN- and AlTiN-coated tools with various cutting parameters based on a central composite design of experiments. In milling operations, Milan et al. [3] proposed an extended Taylor's tool life equation based on the tool life criterion of average flank wear of 0.4 mm when milling the calcium-treated and nontreated mold steels (AISI P20 and P 20 UF steels) using the three coatings TiN-, Al_2O_3-, and TiCN-coated carbide cutting tools. Kuo et al. [4] formulated Taylor's tool life equation as a function of cutting time based on the maximum flank wear criterion of 0.3 mm during milling of superalloy Inconel 718 using uncoated, TiN-, and TiCN-coated tools. In addition, the modified Taylor's equations were used to estimate the tool life as a function of feed per tooth and cutting speed based on the proposed procedure [5]. In turning operation, Taylor's tool life equation was also used to estimate the tool life of cutting tools when machining various workpiece materials, including AISI 52100 steel using polycrystalline cubic boron nitrides [6], AISI 302 stainless steel using carbide inserts of P10 grade

* E-mail: charn_sa@kku.ac.th

© Phacharadit Paengchit and Charnnarong Saikaew 2023. This is an open access article distributed under the Creative Commons Attribution-NonCommercial-NoDerivatives 4.0 License. (http://creativecommons.org/licenses/by-nc-nd/4.0/)

with a triangular shape of 16 mm in side length and 3.18 mm in thickness [7], martensitic stainless steel using TiAlN [8], AISI H13 steel with WC-TiC-Co ultrafine cemented carbide [9], Ti6Al4V (UNS R56400) alloy utilizing with uncoated WC-Co inserts [10], martensitic S41000, and supermartensitic S41426 steels using carbide tools coated with TiC/TiCN/TiN by the chemical vapor deposition coating method [11].

Nomenclature

$\mathbf{R_a}$	Surface roughness (μm)
$\boldsymbol{v}$	Cutting speed (m/min)
$\boldsymbol{T}$	Tool life (min)
$\boldsymbol{f}$	Feed rate (mm/rev)
$\boldsymbol{n}, \boldsymbol{m}$	The exponents of Taylor's tool life equation
$\boldsymbol{c}$	The constant of Taylor's tool life equation
S.D.	Standard deviation
CNC	Computer numerical control
WC	Tungsten carbide
MCS	Monte Carlo simulation

Not only is Taylor's tool life equation developed on the basis of the criterion of tool wear, but it also can be evaluated on the basis of other criteria. Many factors influence tool life, including tool materials, tool shapes, machining operating conditions, coolant types, and workpiece surface quality requirements. Taylor's tool life equation is utilized to describe the relationship between tool life and machining parameters. For example, according to Taylor's tool life model, Chen and Luo [12] successfully demonstrated the relationship between tool wear and chip morphology with an average error of experimental repeatability of 4.5%. This indicated that chip surface chromaticity was used to predict tool wear based on the development of Taylor's tool life equation during the cutting of stainless steel (2316ISO-B MOD) with a TiAlN coated insert. In a drilling operation, the tool life equation was utilized to create a relationship between tool life and cutting speed and feed rate during machining of forging brass with uncoated tungsten carbide (WC) and AlCrN-coated WC tools using the criterion of exit burr height of 0.16 mm [13]. Kovac et al. [14] also proposed an extended Taylor's functional relationship between tool life and cutting speed, feed per tooth, and depth of cut through measurements of tool-workpiece thermocouple temperature during milling of AISI 1060 steel with a carbide insert of 125 mm in diameter. They stated that the proposed method for Taylor's tool life equation was faster work pace and lower cost than the traditional method. Kundrák and Pálmai [15] proposed tool life models, which were modified from Taylor's tool life equation based on the number of turned boreholes in turning internal cylindrical surfaces of $100Cr_6$ hardened steel using cubic boron nitride K10. Meanwhile, the lifetime of a machine component (i.e., the fishing net weaving machine component of a fishing net weaving machine) was evaluated by the weight of material removed from the component during wear tests [16].

Surface quality and dimensional accuracy of machined parts are crucial for many applications. Manufacturers need to evaluate the machinability performances during computer numerical control (CNC) turning of various materials using a variety of tool inserts when a machined workpiece's surface roughness (R_a) begins to degrade and fails to match the customer's requirements for workpiece surface quality, leading to high manufacturing costs. Normally, tool wear increases, resulting in increasing R_a due to vibration of the tool tip at high acceleration [17]. Consequently, R_a can be indirectly used as a criterion for assessing cutting tool deterioration.

This research aims to develop and evaluate the tool life models of Al_2O_3+TiC and TiN+AlCrN during turning of AISI 4140 steel with different cutting speeds and feed rates using Taylor's tool life equation with a maximum R_a of 0.8 μm for the tool life criterion. Monte Carlo simulation (MCS) was also used to evaluate the sensitivity of cutting speed and feed rate to tool life. It has been pointed out that AISI 4140 steel has been extensively used in a wide range of industrial applications including component parts for vehicles such as shafts, crankshafts, gears, connecting rods, and collars as well as machinery parts in the oil and gas industry and other industries like motor shafts, pump

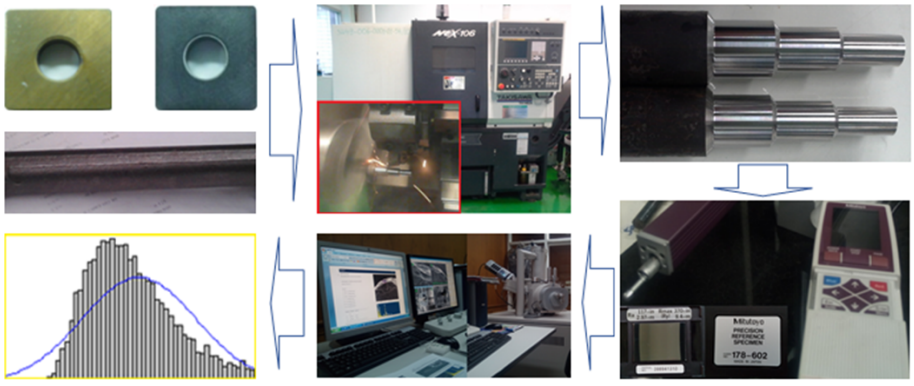

Fig. 1. Overview of the experimental work and the machine samples

shafts, honed cylinder tubes for hydraulic, pneumatic cylinder barrels, bolts, forging die, jigs, and frames due to its toughness, abrasion and impact resistance, and high fatigue strength [18].

2. Research methods

Figure 1 shows an overview of the experimental work and the machined samples for the hard-turning study. The workpiece material was AISI 4140 chromium molybdenum steel bars. The chemical compositions were as follows: 0.47% C, 1.05% Cr, 0.01% P, 0.01% S, 0.26% Si, 0.67% Mn, 0.2% Mo, 0.0042% V, 0.012% Al, and 0.19% Cu. Its hardness value was 58 HRC.

The turning experiments were carried out in a Fanuc CNC lathe machine (Takisawa model: NEX-106). The cutting tools were mixed ceramic insert (Al_2O_3+TiC) (Tungaloy, Japan) and TiN+AlCrN-coated insert. The ISO designation of the inserts and tool holder was SNGA120408TH10 and ASBNR2020K12-A coded external tool holder.

The experiments were carried out on AISI 4140 steel bar samples with two types of tool inserts at three cutting speeds (200, 220, 240 m/min) and three feed rates (0.04, 0.06, 0.08 mm/rev) while keeping the depth of cut constant at 0.1 mm.

A commercial surface roughness measuring tester (Mitutoyo model: Surf test SJ-210) with a cut-off length of 0.8 mm and a sampling length of 5 mm was used to measure R_a. R_a measurements were taken at three different locations on each of the machined workpieces. The maximum R_a of 0.8 µm was set with the customers' requirements for quality acceptance of automotive parts [19]. The wear of the tool insert was investigated using a scanning electron microscope (Hitachi model S-4700) with a 20-kV accelerating voltage.

The turning experiments were carried out to obtain data for tool life models of the two tool inserts. Taylor's equation was used to obtain the relationships between tool life and cutting speed and feed rate of the two tool inserts. The equation is defined as:

$$T(v)^{1/n}(f)^{1/m} = c \tag{1}$$

where v represents cutting speed, T denotes tool life, and f indicates feed rate [20, 21]. The exponents n, m, and the constant c are obtained from Taylor's equation fitting to the observations of turning of AISI 4140 samples using both tool inserts.

Monte Carlo simulation (MCS) is a sampling experiment used for approximating the distribution of an outcome factor that is dependent on various probabilistic input factors [22]. It is regularly used to evaluate the sensitivity of processes in various areas. This method has been used in numerous studies and many application areas since World War II [23]. Marci et al. [24] compared the thin films sputtering yields for low-energy noble gas ions bombardment on MgO and $Mg(OH)_2$ targets in the binary collision approximation. This method demonstrated that the sputtering depends on both the incident particle and the targets. In the cold spray process of mixtures of alumina content and aluminum particles, the effects of particle size, par-

ticle size distribution, and behavior of deposition efficiency were evaluated and compared between the numerical simulation and the experimental data [25]. In the grinding process of machined parts, MCS was adopted to identify the sensitivities in surface roughness of machined parts after obtaining the appropriate operating conditions of wheel speed and feed rate of the grinding process using a central composite design of experiment and response surface methodology [26]. In addition, Kahraman and Öztürk [27] used MCS in sensitivity analyses to evaluate the effects of grinding process parameters on the average surface roughness of the hard-brittle materials [27] and flat glass [28]. To improve the operational reliability of a thermal power plant, Kostić et al. [29] simulated the failure interaction of the system components based on the Weibull probability distribution. In milling operation of aluminum 7075, Kahraman et al. [30] investigated the effect of cutting speed, feed rate, and depth of cut on average surface roughness using Taguchi design of experiment and examined the sensitivity analysis of R_a of the machined parts using MCS. In a turning operation of AISI D2 steel, Sarnobat and Raval [31] evaluated the influence of tool edge geometry and work piece hardness on averages of the tri-axial surface residual stresses, surface roughness, and work hardening in the affected machining region. They studied the sensitivity of the tri-axial stresses and surface roughness of the machine parts to the process parameters by applying MCS. Thomas et al. [32] presented three cases regarding design, development, and implementation of MCS to define a bearing replacement strategy due to bearing failures within a steel-processing industry for a total productive maintenance program. They stated that the bearing replacement strategy contributed a simple approach to significantly improving system reliability and achievement through less downtime and higher cost savings. Timata and Saikaew [13] studied the sensitivity of cutting speed and feed rate to tool life prediction in tool life evaluation by adopting an MCS based on Taylor's tool life equation.

Therefore, MCS was utilized in this study to evaluate tool life predictions. Sensitivity of cutting speed and feed rate to tool life was studied while turning AISI 4140 samples using the criterion of average R_a of 0.8 μm. The simulation was performed by varying cutting speeds below and above the cutting speed of 220 m/min while keeping the feed rate constant at 0.06 mm/rev and by varying feed rates below and above the feed rate of 0.06 mm/rev while keeping the cutting speed constant at 220 m/min. Minitab software package version 16 was used to run MCS.

3. Results and discussion

3.1. Microstructure and tool life analyses

Figures 2(a) and 2(b) illustrate SEM micrographs of Al_2O_3+TiC and TiN+AlCrN inserts at both a low magnification and a high magnification zoomed in the oval region marked in the corresponding low magnification images after turning AISI 4140 steel for 45 min at a cutting speed of 220 m/min and a feed rate of 0.06 mm/rev by keeping the depth of cut constant at 0.1 mm. Flank wear and crater wear as well as adhered workpiece material on the worn cutting tool surface appear on the cutting edges of the two inserts. The wear was nonuniform with a concave profile. The horizontal widths of concave worn regions were longer than 200 μm for both inserts, indicating extensive wear of the cutting edges. Furthermore, the concave region on the cutting edge of the TiN+AlCrN insert was deeper than that of the Al_2O_3+TiC insert, indicating severe wear of the cutting edge of TiN+AlCrN during machining of the hard steel.

At the high magnification of the SEM images, the worn regions were quite rough, exhibiting random-shaped indentations and protrusions. In addition, there were some micron-sized particles that adhered to the worn regions, suggesting possible attrition of the workpiece material. Severe abrasion caused the workpiece material to adhere to the tool surface. Wear debris and chips generated on the cutting edge of TiN+AlCrN were greater than those of Al_2O_3+TiC. These features are attributed to the fact that the harder tool insert material abrades the softer workpiece surface in compressive and shear directions causing the formation of particles and chips [19]. The results indicated that the volume

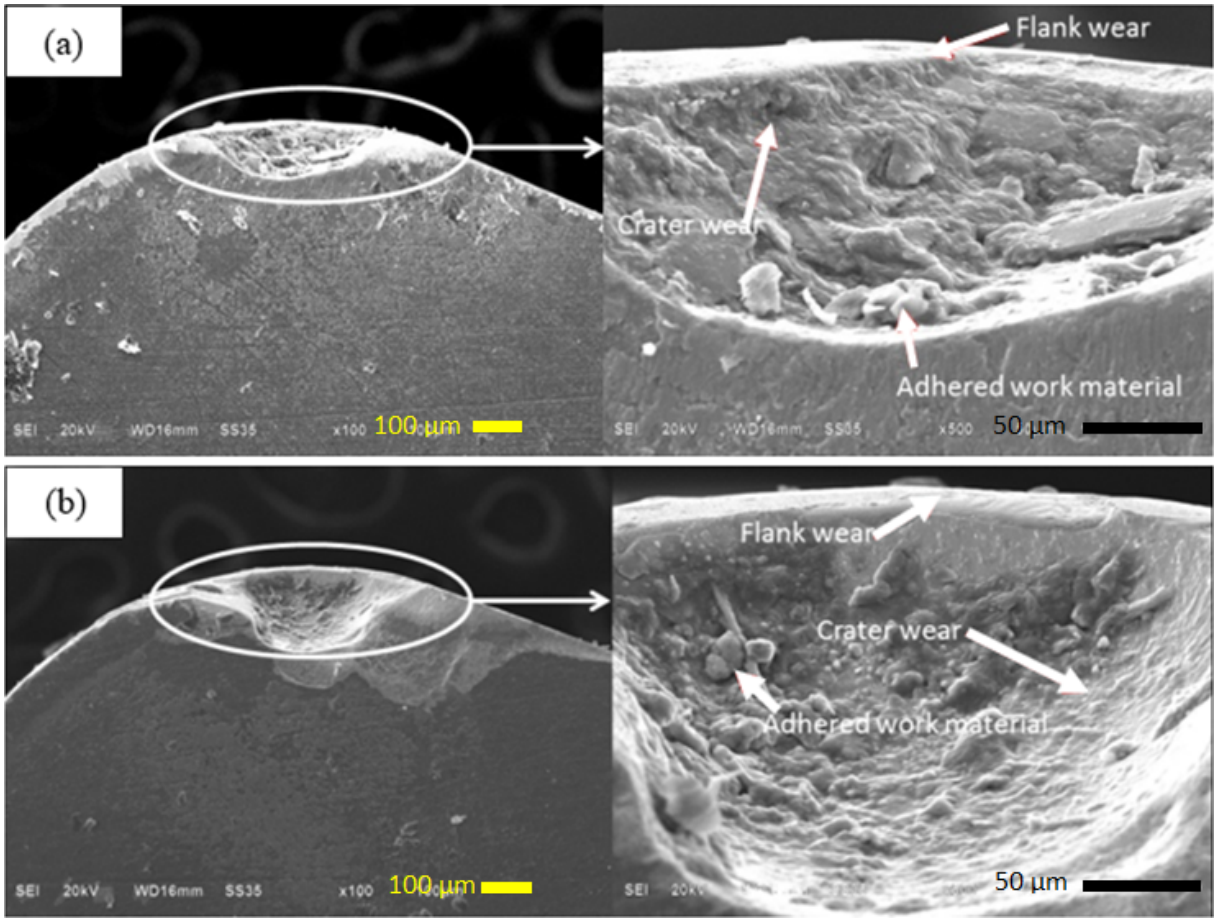

Fig. 2. SEM images of (a) Al_2O_3+TiC and (b) TiN+AlCrN worn inserts after turning for 45 min

of material removed from the TiN+AlCrN tool insert was greater than that from the Al_2O_3+TiC tool insert based on the deeper crater wear on the cutting edge during machining at the same operating condition. Hence, the Al_2O_3+TiC had better wear resistance than TiN+AlCrN due to the distinct mechanical properties of the base materials and the tool inserts.

Figures 3(a) and (b) show SEM images of Al_2O_3+TiC and TiN+AlCrN inserts at both low and high magnification zoomed in on the oval regions marked in the corresponding low-magnification images after turning AISI 4140 steel for more than 75 min at a cutting speed of 220 m/min and a feed rate of 0.06 mm/rev by keeping the depth of cut constant at 0.1 mm. They show catastrophic failure modes of inserts on the cutting edges where noses completely disappear due to crack and chipping. The tool fracture results from high stress and a large amount of cutting heat due to the abrasion between the tool cutting edge, especially at the nose region, and the workpiece, leading to material cracking and chipping.

Table 1 shows the results of R_a values of the machined samples at different cutting times after the turning operation at various machining conditions using Al_2O_3+TiC and TiN+AlCrN tool inserts. Figure 4 shows the relationships between average R_a values and cutting time at cutting speeds of 200, 220, and 240 m/min while keeping the feed rate constant at 0.06 mm/rev during turning of the workpiece samples using Al_2O_3+TiC and TiN+AlCrN tool inserts, respectively. Likewise, Figure 5 illustrates the relationships between average R_a values and cutting time at feed rates of 0.04, 0.06, and 0.08 mm/rev while maintaining a

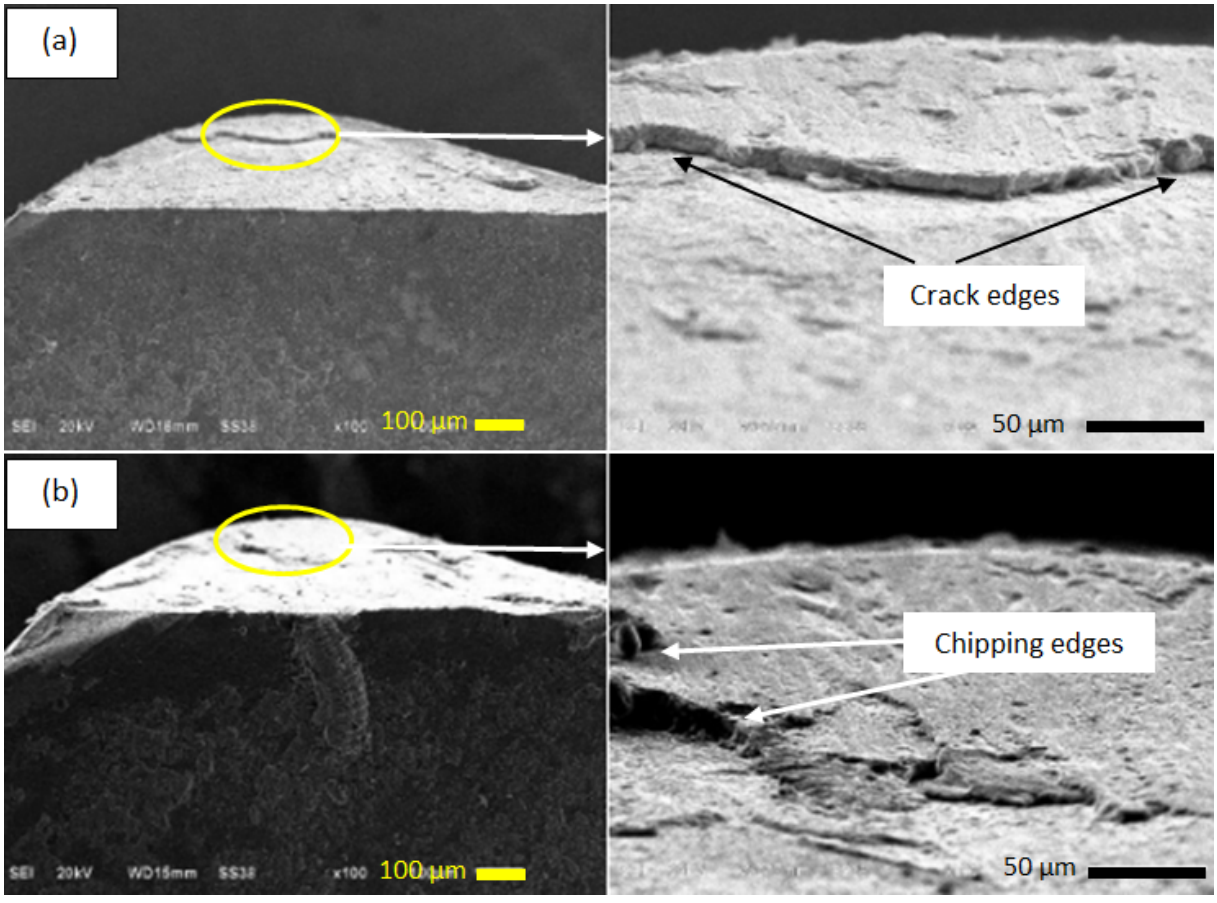

Fig. 3. SEM images of (a) Al_2O_3+TiC and (b) TiN+AlCrN failed inserts after turning for more than 75 min

Table 1. Results of R_a (in µm) values of the machined samples at different cutting times

Cutting time (min)	Al_2O_3+TiC						TiN+AlCrN					
	Cutting speed (m/min) (Holding feed rate constant at 0.06 mm/rev)			Feed rate (mm/rev) (Holding cutting speed constant at 220 m/min)			Cutting speed (m/min) (Holding feed rate constant at 0.06 mm/rev)			Feed rate (mm/rev) (Holding cutting speed constant at 220 m/min)		
	200	220	240	0.04	0.06	0.08	200	220	240	0.04	0.06	0.08
5	0.594	0.610	0.635	0.532	0.610	0.634	0.612	0.634	0.691	0.610	0.634	0.683
5	0.561	0.606	0.656	0.556	0.606	0.673	0.608	0.638	0.673	0.620	0.638	0.698
5	0.534	0.608	0.647	0.545	0.608	0.657	0.616	0.641	0.680	0.640	0.641	0.687
15	0.583	0.646	0.713	0.597	0.646	0.689	0.728	0.701	0.759	0.668	0.701	0.712
15	0.602	0.645	0.734	0.566	0.645	0.741	0.684	0.715	0.772	0.658	0.715	0.754
15	0.563	0.653	0.720	0.579	0.653	0.732	0.691	0.718	0.769	0.678	0.718	0.761
30	0.637	0.732	0.853	0.643	0.732	0.857	0.775	0.835	0.919	0.774	0.835	1.064
30	0.629	0.713	0.824	0.621	0.713	0.837	0.769	0.828	0.906	0.723	0.828	0.937
30	0.631	0.698	0.810	0.639	0.698	0.823	0.793	0.821	0.912	0.734	0.821	0.986
45	0.796	0.850	0.961	0.801	0.850	0.990	0.864	1.030	1.130	0.876	1.030	1.302
45	0.771	0.852	0.927	0.778	0.852	1.064	0.854	0.998	1.138	0.857	0.998	1.282
45	0.782	0.840	0.945	0.764	0.840	1.107	0.879	0.981	1.122	0.869	0.981	1.292
60	0.938	0.945	1.097	0.920	0.945	1.217	1.162	1.173	1.293	1.018	1.173	1.489
60	0.979	0.989	1.109	0.897	0.989	1.120	1.127	1.153	1.280	1.031	1.153	1.491
60	0.901	0.918	1.073	0.883	0.918	1.327	1.136	1.149	1.253	1.011	1.149	1.487
75	1.108	1.097	1.142	1.092	1.097	1.378	1.474	1.474	1.625	1.253	1.474	1.881
75	1.058	1.112	1.198	1.035	1.112	1.392	1.513	1.342	1.488	1.271	1.342	1.687
75	1.074	1.096	1.124	1.066	1.096	1.346	1.486	1.472	1.581	1.213	1.472	1.774

constant cutting speed of 220 m/min. For all cutting speeds and feed rates, the average R_a of the sample surfaces increased monotonically with increasing cutting time for both tool inserts. The average R_a met the criterion of 0.8 μm in the ranges of cutting time from 20 min to 45 min. The results also indicated that turning at higher cutting speeds and feed rates increased the average R_a for both tool inserts. At each cutting time, however, R_a values were not dramatically different when turning the workpieces with different cutting speeds using both inserts. On the other hand, the R_a values were highly increased with the increasing feed rate at higher cutting times for both inserts.

Based on the observations of average R_a in Figures 4 and 5 with the R_a remaining below 0.8 μm, the tool life equation for the mixed ceramic insert (Al_2O_3+TiC) can be obtained as

$$T = 7.1178 \times 10^7 (v^{-3.0581})(f^{-0.7829}) \qquad (2)$$

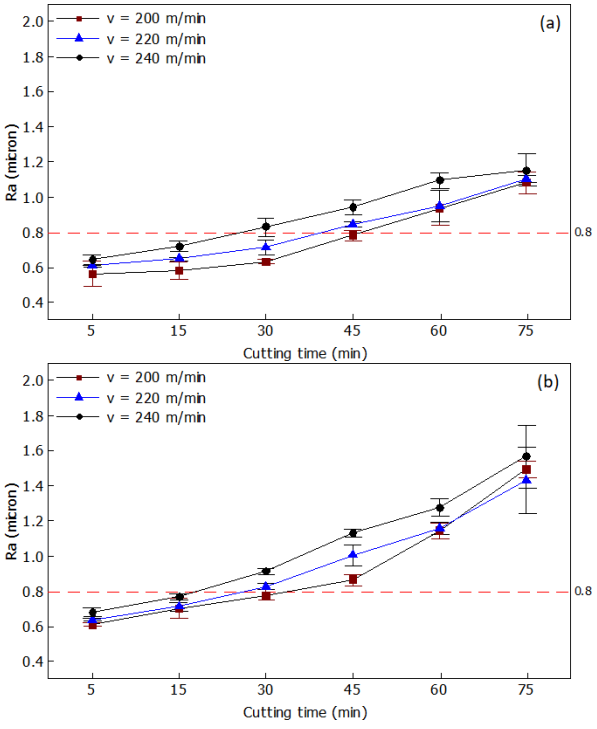

Fig. 4. R_a versus cutting time during turning workpiece samples using (a) Al_2O_3+TiC and (b) TiN+AlCrN tool inserts by varying cutting speeds

For the TiN+AlCrN coated insert, the tool life equation can be expressed as

$$T = 8.2015 \times 10^7 (v^{-3.1847})(f^{-0.8376}) \qquad (3)$$

Eqs. (2) and (3) were employed to generate tool life predictions for the mixed ceramic insert and

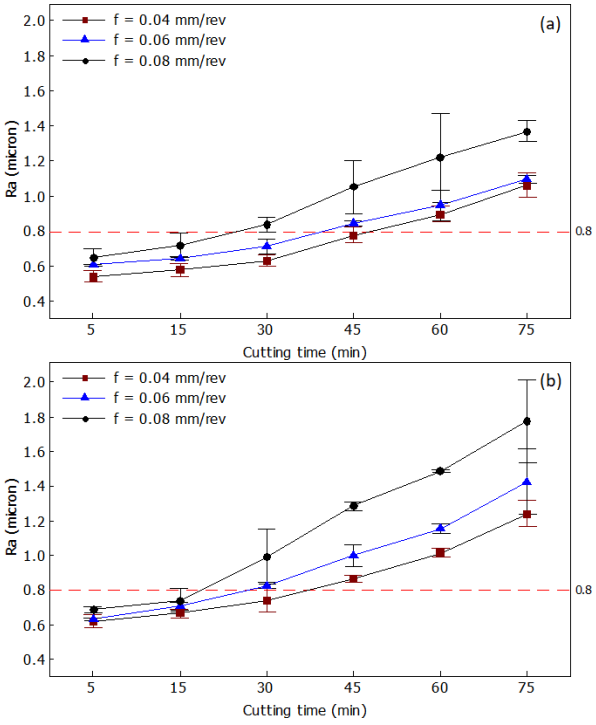

Fig. 5. R_a versus cutting time during turning workpiece samples using (a) Al_2O_3+TiC and (b) TiN+AlCrN tool inserts by varying feed rates

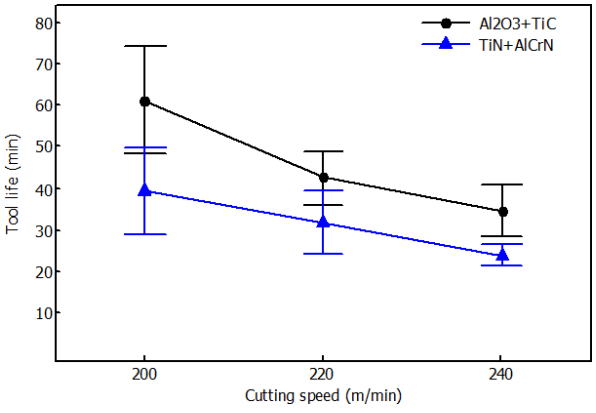

Fig. 6. A plot of the relationship between predicted tool life values and cutting speed while keeping the feed rate constant at 0.06 mm/rev

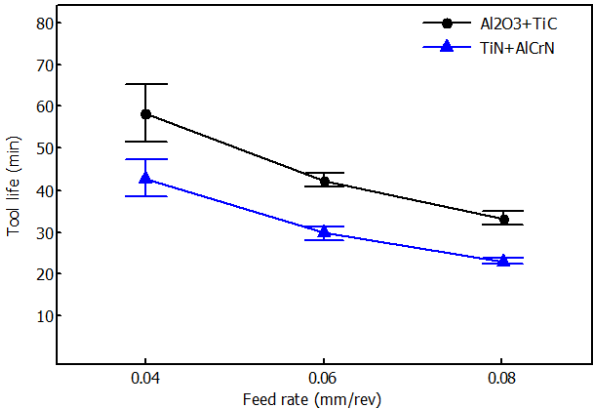

Fig. 7. A plot of the relationship between predicted tool life values and feed rate while keeping the cutting speed constant at 220 m/min

Table 2. Predicted tool life values of the two tool inserts by varying cutting speeds −10%, −5%, 5%, and 10% from 220 m/min while keeping the feed rate constant at 0.06 mm/rev

% Change	Al_2O_3+TiC		TiN+AlCrN	
	Average	S.D.	Average	S.D.
−10	65.92	25.37	46.65	18.33
−5	55.75	20.08	38.32	14.27
5	40.33	12.74	27.42	9.00
10	34.66	10.36	23.48	7.73

the coated insert, respectively. Figure 6 presents the relationship between predicted tool life and cutting speed when the feed rate was kept constant at 0.06 mm/rev, whereas Figure 7 exhibits the tool life versus feed rate when the cutting speed was maintained constant at 220 m/min. Obviously, increasing the cutting speed and feed rate decreased tool life of both inserts. Moreover, the Al_2O_3+TiC showed longer tool life than the TiN+AlCrN at various cutting speeds and feed rates.

3.2. Simulation analysis

Taken from the results of am MCS performed by generating 10,000 simulated values from normal distribution, Figures 8 and 9 show histograms of tool life values of Al_2O_3+TiC tool inserts by varying cutting speeds below and above the cutting speed of 220 m/min while keeping the feed rate constant at 0.06 mm/rev. Table 2 presents the comparisons of tool life values of the two inserts based on MCS results. Apparently, the average tool life of Al_2O_3+TiC was approximately 40% larger than that of TiN+AlCrN, whereas the variation of tool life values of TiN+AlCrN was lower than that of Al_2O_3+TiC.

Similarly, Figures 10 and 11 illustrate histograms of tool life values of Al_2O_3+TiC tool inserts by varying feed rates below and above the feed rate of 0.06 mm/rev while keeping the cutting speed constant at 220 m/min. Table 3 presents the comparisons of tool life values of the two inserts based on MCS results from Figures 10 and 11. The average tool life of Al_2O_3+TiC was approximately 45% larger than that of TiN+AlCrN. Likewise, variation of tool life values of TiN+AlCrN was slightly lower than that of Al_2O_3+TiC.

3.3. Discussion of findings

By increasing cutting speed, tool life of Al_2O_3+TiC was decreased slightly more than that of TiN+AlCrN based on the relationship between predicted tool life values and cutting speed by keeping the feed rate constant at 0.06 mm/rev. Additionally, the variation of tool life values was

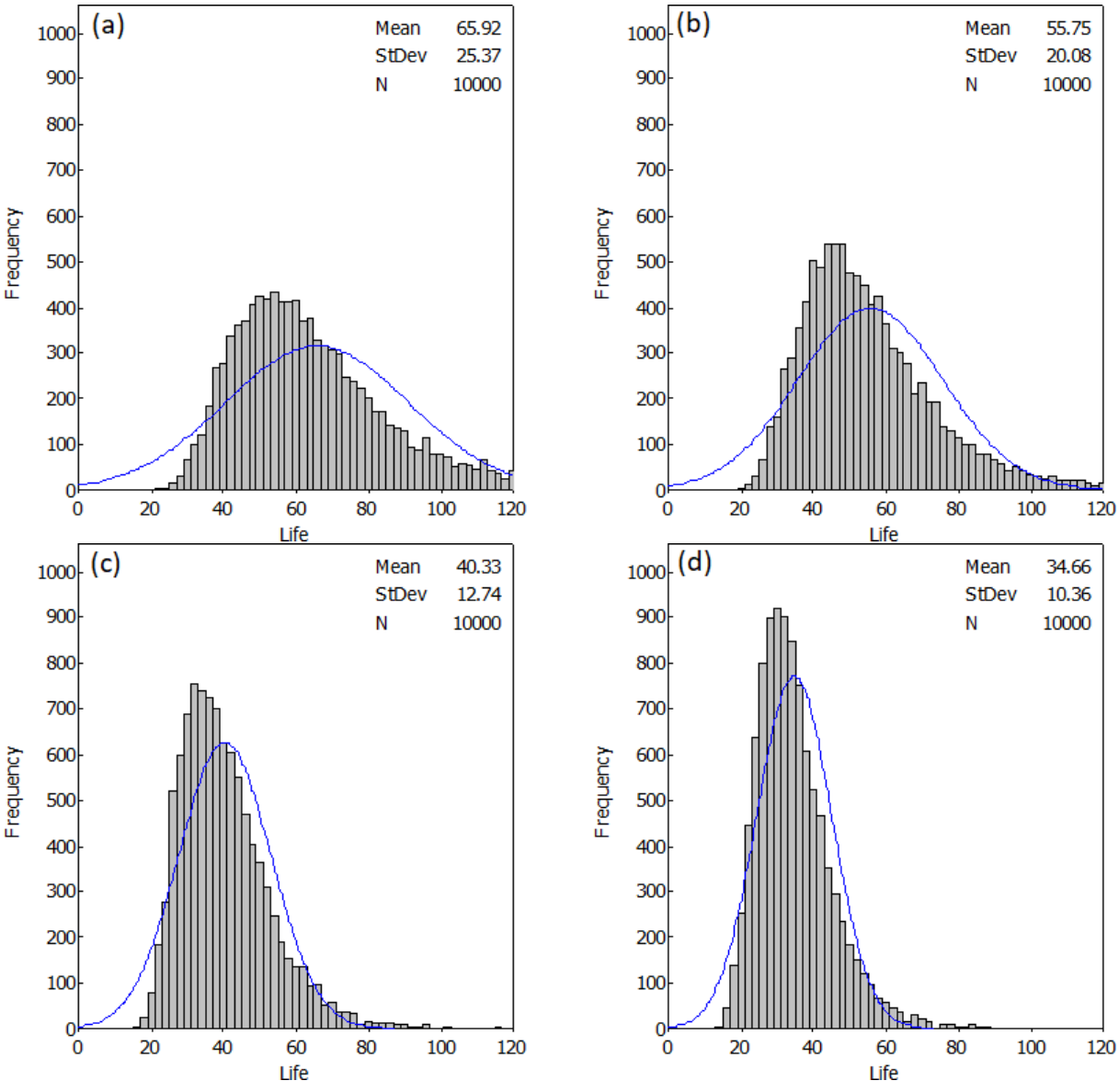

Fig. 8. Predicted tool life values of Al_2O_3+TiC by varying cutting speeds (a) −10%, (b) −5%, (c) 5%, and (d) 10% from 220 m/min while keeping the feed rate constant at 0.06 mm/rev

Table 3. Predicted tool life values of the two tool inserts by varying feed rates −10%, −5%, 5%, and 10% from 0.06 mm/rev when keeping the cutting speed constant at 220 m/min

% Change	Al_2O_3+TiC		TiN+AlCrN	
	Average	S.D.	Average	S.D.
−10	48.46	4.35	33.13	3.22
−5	46.36	3.97	31.65	2.90
5	42.79	3.28	29.02	2.41
10	41.30	3.01	27.91	2.18

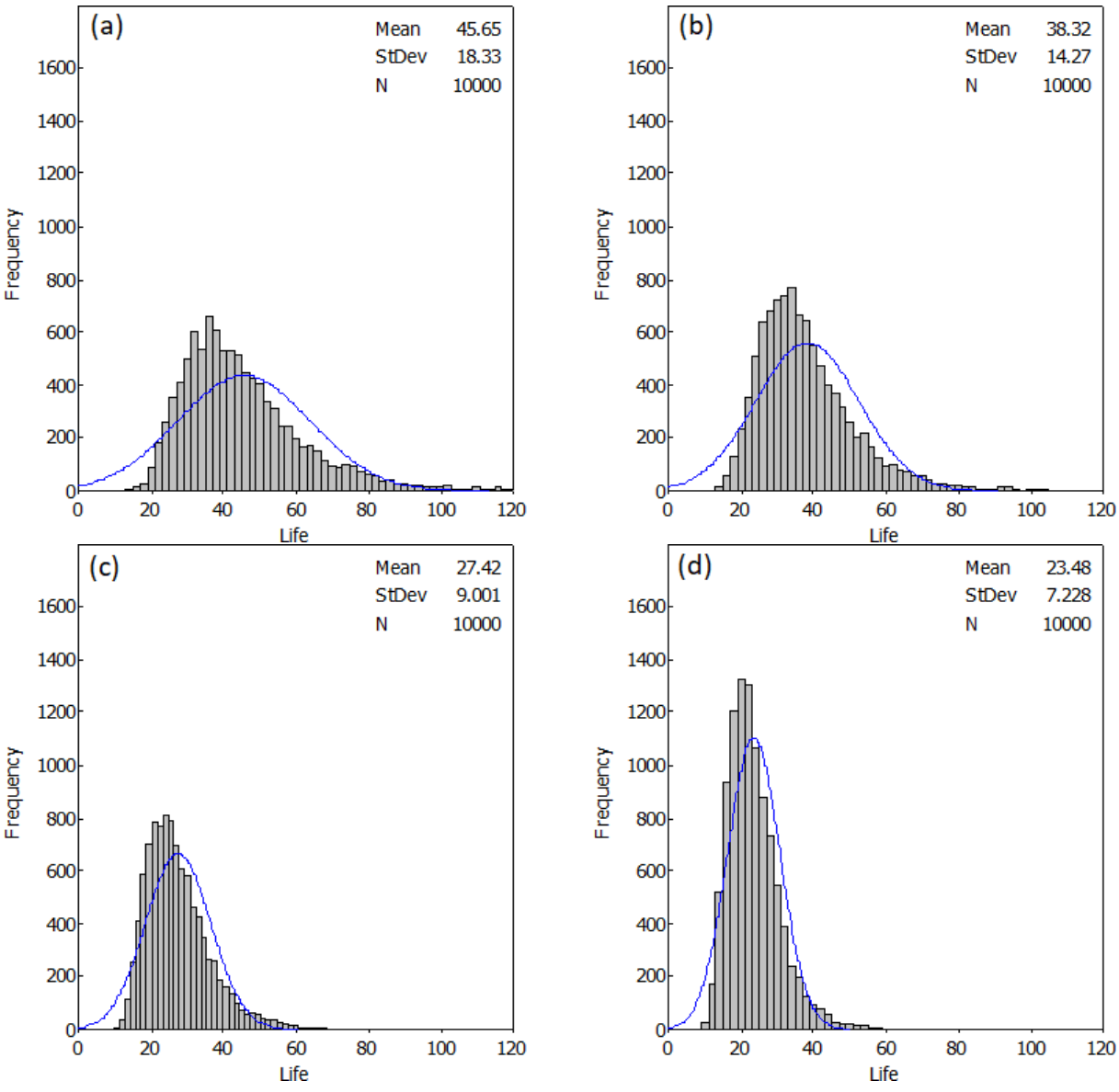

Fig. 9. Predicted tool life values of TiN+AlCrN by varying cutting speeds (a) −10%, (b) −5%, (c) 5%, and (d) 10% from 220 m/min while keeping the feed rate constant at 0.06 mm/rev

smaller when increasing cutting speed for both inserts. The results confirmed that Al_2O_3+TiC has longer tool life than TiN+AlCrN. The results of this study agreed with the findings of other studies. Masuda et al. (1994) stated that Al_2O_3+TiC has the best wear resistance compared to alumina and other alumina-based cutting inserts when turning the austempered ductile iron (ADI) at the cutting speed of 100 m/min, feed rate of 0.1 mm/rev and depth of cut of 1 mm under dry condition [33]. Additionally, by increasing cutting speed, the wear rate of Al_2O_3+TiC increased linearly on the double logarithmic diagram, whereas the wear rates of alumina and the other alumina-based inserts increased gradually. They also confirmed that the tool life of Al_2O_3+TiC was longer when turning the ADI at least 250 m/min [33]. This is attributed to the fact that mechanical properties including fracture toughness, transverse strength, and hardness were improved by 12.5%, 12.5%, and 11.1%,

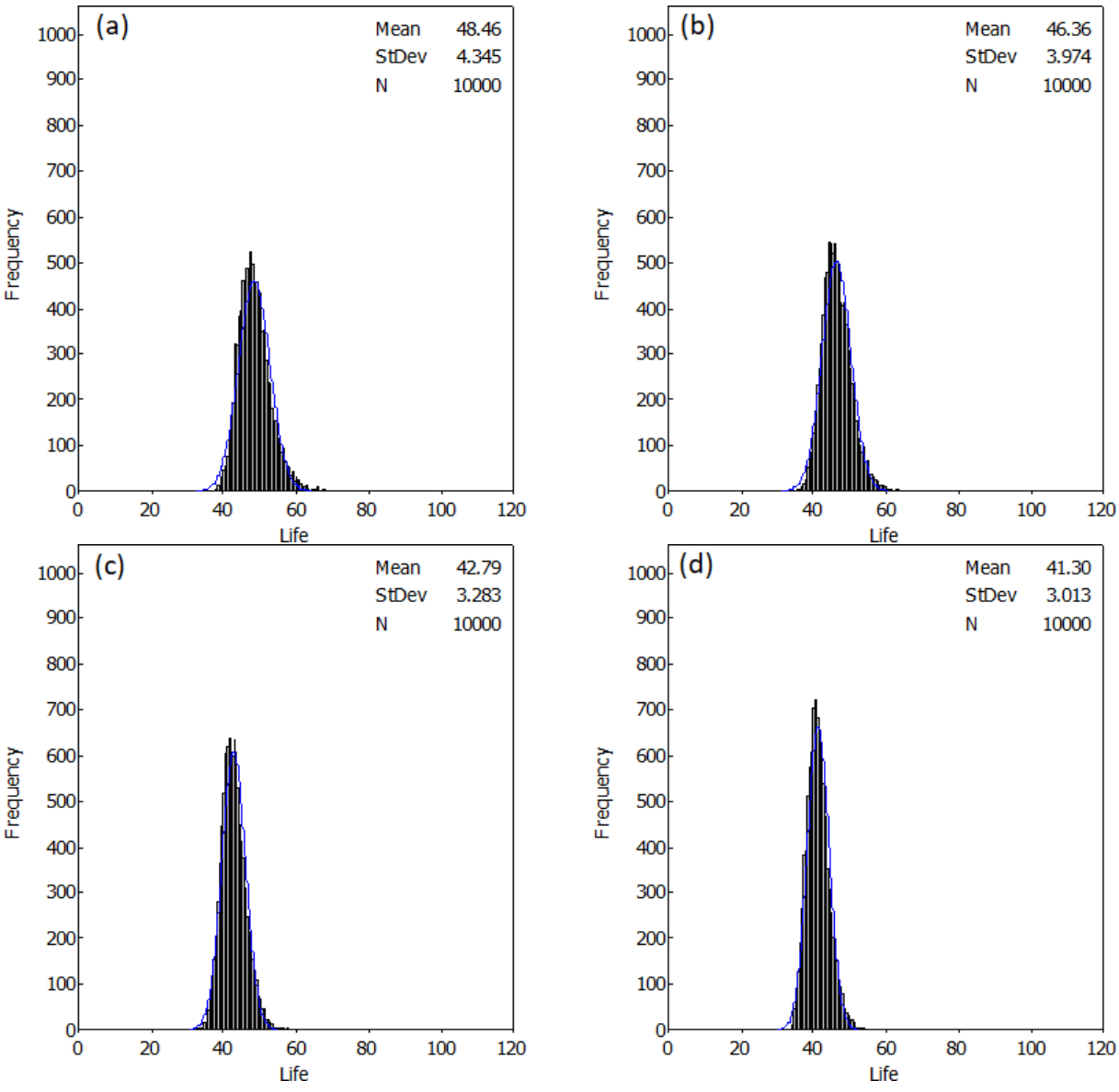

Fig. 10. Predicted tool life values of Al_2O_3+TiC by varying feed rates (a) −10%, (b) −5%, (c) 5%, and (d) 10% from 0.06 mm/rev while keeping the cutting speed constant at 220 m/min

respectively, by adding TiC in Al_2O_3. Meanwhile, Fernandez-Valdivielso et al. [34] stated that Al_2O_3+TiC has the best wear resistance compared to Al_2O_3+SiCw and other inserts during turning of the ADI at a cutting speed of 200 m/min, feed rate of 0.1 mm/rev, and depth of cut of 1.5 mm.

The results of MCS revealed that variations of tool life values induced by varying cutting speeds were highly sensitive compared to the tool life values resulting from varying feed rates for both inserts. Furthermore, the variation of tool life values of Al_2O_3+TiC dramatically increased (by 5%) with decreasing cutting speed from 220 m/min to 210 m/min and 200 m/min (by 10%). The tool life of Al_2O_3+TiC can reach 120 min with a cutting speed of less than 220 m/min while that of TiN+AlCrN can barely reach as far as 120 min with a cutting speed of less than 220 m/min. On the other hand, the simulation results showed that the tool life of Al_2O_3+TiC can reach as high as 80 min with a cut-

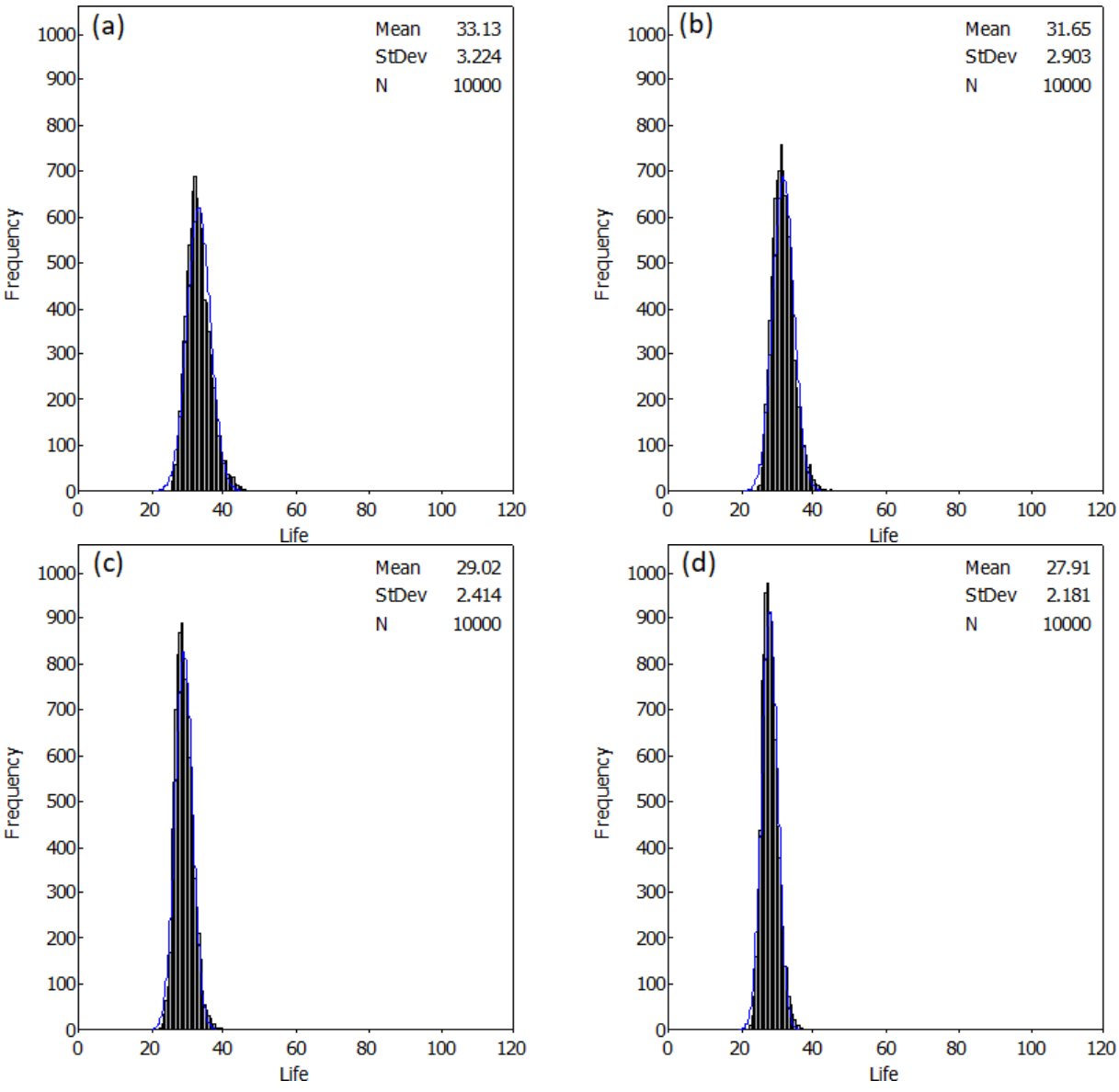

Fig. 11. Predicted tool life values of TiN+AlCrN by varying feed rates (a) −10%, (b) −5%, (c) 5%, and (d) 10% from 0.06 mm/rev when keeping the cutting speed constant at 220 m/min

ting speed of more than 220 m/min while that of TiN+AlCrN can barely reach 60 min with a cutting speed of more than 220 m/min.

The findings also indicated that the variability of tool life values for Al_2O_3+TiC was not significantly changed when feed rate decreased to below 0.06 mm/rev by 5% and 10% while keeping the cutting speed constant at 220 m/min. Tool life was in the range of 40 to 60 min with decreasing feed rate below 0.06 mm/rev by 5% and 10%. On the other hand, the tool life values ranged from 30 to 50 min when turning AISI 4140 steel using Al_2O_3+TiC with an increasing feed rate above 0.06 mm/rev by 5% and 10%.

Moreover, the simulation results showed that the variability of tool life values for TiN+AlCrN did not change when the feed rate decreased below 0.06 mm/rev by 5% and 10% while feed rate increased above 0.06 mm/rev by 5% and 10%. The simulation results also indicated that the tool life

values ranged from 20 to 40 min while turning the TiN+AlCrN samples with a feed rate that increased above 0.06 mm/rev by 5% and 10%.

The practical implications of the simulation study suggest that manufacturers need to pay attention to how much the cutting speed and feed rate vary during the turning of AISI 4140 steel with the two cutting inserts. Manufacturing at the appropriate cutting speed, feed rate, and other cutting parameters can move towards improving production sustainability. Xiong et al. [9] stated that reliability analysis of turning tool life provides a theoretical igrounding for selecting the appropriate machining process parameters and tool replacement strategies.

4. Conclusion

The tool life performance of Al_2O_3+TiC and TiN+AlCrN tool inserts were studied for dry turning of AISI 4140 steel. Based on the comparison of test results of Taylor's tool life equations and MCS, the following conclusions could be drawn:

- The machined part's surface quality was effectively employed as a criterion for monitoring cutting tool deterioration.
- Reducing cutting speed and feed rate can prolong the tool life of both tool inserts.
- Al_2O_3+TiC exhibited longer tool life than TiN+AlCrN in turning operations at different cutting speeds and feed rates.
- Based on the MCS results, the average tool life of Al_2O_3+TiC was approximately 40% greater than that of TiN+AlCrN when varying cutting speeds below and above a cutting speed of 220 m/min when keeping the feed rate constant at 0.06 mm/rev.
- Likewise, the average tool life of Al_2O_3+TiC was approximately 45% greater than that of TiN+AlCrN when varying feed rates below and above the feed rate of 0.06 mm/rev when keeping the cutting speed constant at 220 m/min.
- The MCS results showed that tool life variations while varying cutting speeds were more sensitive than those when varying feed rates for both tool inserts.
- The practical implications are that manufacturers can more easily evaluate tool life values of the two cutting inserts in turning operations at different cutting parameters as well as for other cutting tools for CNC machines, including milling and drilling machines.

References

[1] John R, Lin R, Jayaraman K, Bhattacharyya D. Modified Taylor's equation including the effects of fiber characteristics on tool wear when machining natural fiber composites. Wear. 2021;468–469: No. 203606, doi: 10.1016/j.wear.2020.203606.

[2] Farid AA, Sharif S, Idris MH. Performance and wear mechanisms of uncoated, TiAlN, and AlTiN-coated carbide tools in high-speed drilling of Al-Si alloy. Int J Adv Manuf Technol. 2021;113:2671–84. doi: 10.1007/s00170-021-06663-w.

[3] Milan JCG, Machado AR, Tomaz IV, da Silva LRR, Barbosa CA, Mia M, Pimenov DY. Effects of calcium-treatment of a plastic injection mold steel on the tool wear and power consumption in slot milling. J Mater Res Technol. 2021;13:1103–14, doi: 10.1016/j.jmrt.2021.05.021.

[4] Kuo CP, Su SC, Chen SH. Tool life and surface integrity when milling inconel718 with coated cemented carbide tools. J Chin Inst Eng, Trans Chin Inst Eng, Series A. 2021;33(6):915–22. doi: 10.1080/02533839.2010.9671680.

[5] Santos ALB, Dos Duarte MAV, Abrao AM, Machado AR. An optimization procedure to determine the coefficients of the extended Taylor's equation in machining. Int J Mach Tools Manuf. 1999;39(1):17–31, doi: 10.1016/S0890-6955(98)00025-X.

[6] Poulachon G, Moisan A, Jawahir IS. Tool-wear mechanisms in hard turning with polycrystalline cubic boron nitride tools. Wear. 2001;250:576–86. doi: 10.1016/S0043-1648(01)00609-3.

[7] El-Tamimi AM, El-Hossainny TM. Investigating the tool life, cutting force components, and surface roughness of AISI 302 stainless steel material under oblique machining. Mater Manuf Proc. 2008;23:427–38. doi: 10.1080/10426910801974846.

[8] Kurniawan D, Yusof NM, Sharif S. Hard machining of stainless steel using wiper coated carbide: tool life and surface integrity. Mater Manuf Proc. 2010;25:370–377. doi: 10.1080/10426910903179930.

[9] Xiong J, Guo Z, Yang M, Wan W, Dong G. Tool life and wear of WC–TiC–Co ultrafine cemented carbide during dry cutting of AISI H13 steel. Ceram Int. 2013;39:337–46, doi: 10.1016/j.ceramint.2012.06.031.

[10] Batista M, Davim P, Salguero J, Gomez-Parra A, Marcos M. Taylor's model based analysis of turning in-

serts tool-life in the dry turning of UNS R56400 alloy. ASME IMECE. 2014; 1. No. 111737, doi: 10.1115/IMECE2014-38710.

[11] Correa JG, Schroeter RB, Machado AR. Tool life and wear mechanism analysis of carbide tools used in the machining of martensitic and supermartensitic stainless steels. Tribol Int. 2017;105:102–17. doi: 10.1016/j.triboint.2016.09.035.

[12] Chen SH, Luo ZR. Study of using cutting chip color to the tool wear prediction. Int J Adv Manuf Technol. 2020;109:823–39. doi: 10.1007/s00170-020-05354-2.

[13] Timata M, Saikaew C. Experimental and simulation study on tool life models in drilling of forging brass using uncoated-WC and AlCrN coated-WC tools. Coatings. 2019;9(853). doi: 10.3390/coatings9120853.

[14] Kovac P, Gostimiroviv M, Rodic D, Savkovic B. Using the temperature method for the prediction of tool life in sustainable production. Meas: J Int Meas Confed. 2019;133:320–7. doi: 10.1016/j.measurement.2018.09.074.

[15] Kundrák J, Pálmai Z. Application of general tool-life function under changing cutting conditions. Acta Polytech. Hung. 11(2):61–76. doi: 10.10700/aph.11.02.2014.02.4.

[16] Srisattayakul P, Saikaew C, Wisisoraat A. Effects of hard chrome and MoN-coated stainless steel on wear behavior and tool life model under two-body abrasion wear testing. Metalurgija. 2017;56(3,4):371–4.

[17] Vasanth XA, Paul PS, Lawrance G, Varadarajan AS. Vibration control techniques during turning process: a review. Aust J Mech Eng. 2017;19:221–41. doi: 0.1080/144848846.2019.1585224.

[18] Aouici H, Elbah M, Yallese MA, Fnides B, Meddour I, Benlahmidi S. Performance comparison of wiper and conventional ceramic inserts in hard turning of AISI 4140 steel: analysis of machining forces and flank wear. Int J Adv Manufa Technol. 2016;87(5–8):2221–44. doi: 10.1007/s00170-016-8567-7.

[19] Saikaew C, Paengchit P, Wisitsoraat A. Machining performances of TiN+AlCrN coated WC and Al_2O_3+TiC inserts for turning of AISI 4140 steel under dry condition. J Manuf Proc. 2020;50:412–20. doi: 10.1016/j.jmapro.2019.12.057.

[20] Taylor FW. On the art of cutting metals. Trans ASME. 1907;28:31–279.

[21] Shaw MC, Cookson JO. Metal cutting principles. Oxford, UK: Oxford University Press; 2005.

[22] Evans JR, Olson DL. Introduction to simulation and risk analysis. Upper Saddle River, NJ, USA: Prentice Hall; 2002.

[23] Law AM, Kelton WD. Simulation modeling and analysis. Second Ed. New York: McGraw-Hill, Inc.; 1991.

[24] Marci ME, Moultif R, Lahlou S, Rochd S, Dezairi A. Monte Carlo simulations of MgO and $Mg(OH)_2$ thin films sputtering yields by noble gas ion bombardment in plasma display panel PDP. Nucl Inst Methods Phys Res B. 2018;430:72–8. doi: 10.1016/j.nimb.2018.05.046.

[25] Klinkov SV, Kosarev VF. Monte Carlo simulation of the cold spray process of mixtures of metal and ceramic powders. J Therm Spray Technol. 2021;30:1081–92. doi: 10.1007/s11666-021-01176-0.

[26] Kahraman MF, Öztürk S. Uncertainty analysis of cutting parameters during grinding based on RSM optimization and Monte Carlo simulation. Mater Test. 2019;61(12):1215–9. doi: 10.3139/120.111443.

[27] Kahraman MF, Öztürk S. Experimental study of newly structural design grinding wheel considering response surface optimization and Monte Carlo simulation. Meas: J Int Meas Confed. 2019;147: No. 106825, doi: 10.1016/j.measurement.2019.07.053.

[28] Öztürk S, Kahraman MF. Modeling and optimization of machining parameters during grinding of flat glass using response surface methodology and probabilistic uncertainty analysis based on Monte Carlo simulation. Meas: J Int Meas Confed. 2019;145:274–91. doi: 10.1016/j.measurement.2019.05.098.

[29] Kostić D, Milošević D, Stefanović S, Jovanov G, Cvejić R. Improving the operational; reliability model of the "Nikola Tesla-Block A" Therma; power plant system by applying an integrated maintenance model. Trans FAMENA. 2019;38(1):79–94. doi: 10.21278/TOF.43106.

[30] Kahraman MF, Bilge H, Öztürk S. Uncertainty analysis of milling parameters using Monte Carlo simulation, the Taguchi optimization method and data-driven modeling. Mater Test. 2019;61(5):477–83. doi: 10.3139/120.111344.

[31] Sarnobat SS, Raval HK. Experimental investigation and analysis of the influence of tool edge geometry and work piece hardness on surface residual stresses, surface roughness and work-hardening in hard turning of AISI D2 steel. Meas: J Int Meas Confed. 2019;131:235–60. doi: 10.1016/j.measurement.2018.08.048.

[32] Thomas AJ, Chad J, John E, Davis A, Francis M. Defining a bearing replacement strategy using Monte Carlo methods. Int J Qual Reliab Manag. 2010;28(2):155–68, doi: 10.1108/02656711111101737.

[33] Masuda M, Sato T, Kori T, Chujo Y. Cutting performance and wear mechanism of alumina-based tools when machining austempered ductile iron. Wear. 1994;174:147–53, doi: 10.1016/0043-1648(94)90096-5.

[34] Fernandez-Valdivielso A, López de Lacalle LN, Fernandez-Lucio P, Gonzalez H. Turning of austempered ductile iron with ceramic tools. Proc Inst Mechan Engi, Part B: J Eng Manuf. 2021;235:484–93, doi: 10.1177/0954405420957154.

Received 2023-01-20
Accepted 2023-08-22